Supporting Information for

Coseismic rupture model and tectonic implications of January 7, 2022, Menyuan Mw 6.6 earthquake constraints from InSAR observation and field investigation

Yongsheng Li[1], Wenliang Jiang[1], Yujiang Li[1*], Wenhao Shen[1], Zhongtai He[1], Bingquan Li[2], Qiang Li[1], Qisong Jiao[1] and Yunfeng Tian[1]

[1] National Institute of Natural Hazards, Ministry of Emergency Management of China

[2] School of Automation, China University of Geoscience, Wuhan, 430074, China

*Correspondence: yujiangli@ninhm.ac.cn

Introduction

In the supporting information, we present correction of the tropospheric delay errors and terrain-correlated atmospheric phase delay (TCAD) (Fig. S1), the orbit errors correction for descending track 33 and ascending tracking 128 (Fig. S2), the long wavelength phase errors correction for the pixel offset tracking in range direction (Fig. S3), the uncertainties and trade-offs for the nonlinear inversion computed using Monte Carlo analysis (Fig. S4). The Tab. S1 present the focal mechanisms and rupture parameters from different studies, Tab. S2 shows the Sentinel-1 TOPS mode data used in this paper and Tab. S3 shows the parameters in the stratified viscoelastic Burgers model in this paper.

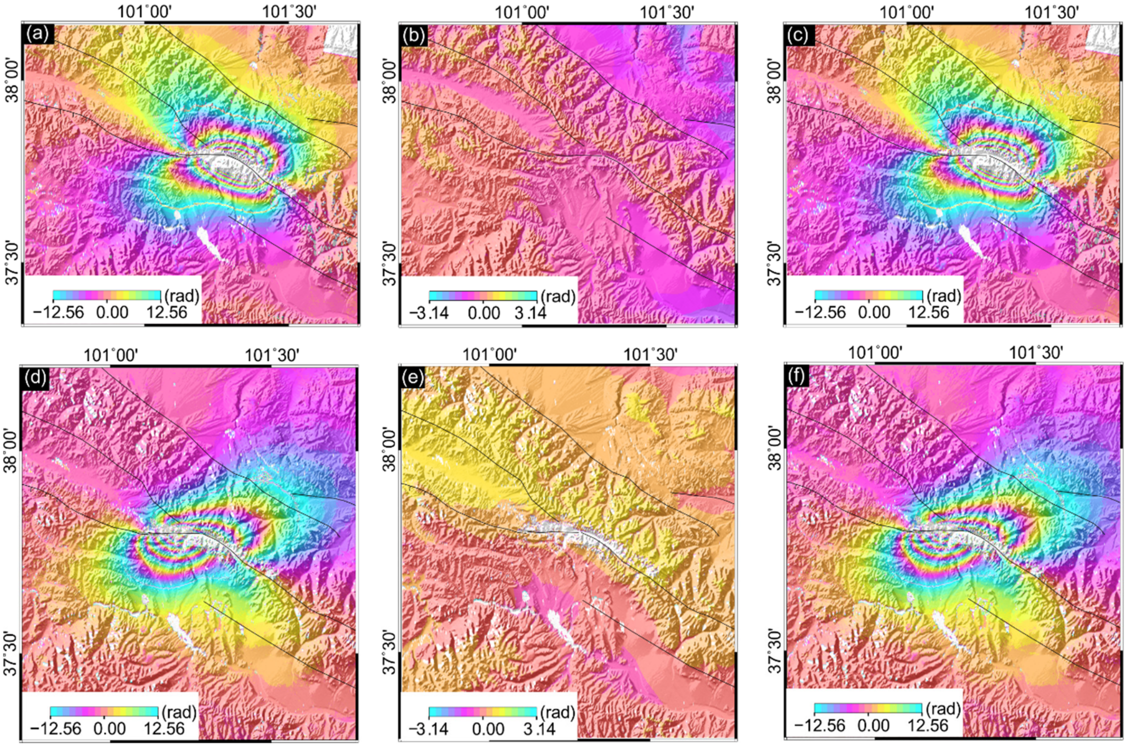

Figure S1. Correction for the tropospheric delay errors and terrain-correlated atmospheric phase delay (TCAD), the external atmospheric delay product from Generic Atmospheric Correction Online Service for InSAR (GACOS). (a) is the original unwrapped coseismic interferogram from Sentinel-1 descending track 33. (b) Modelled atmospheric phase delay for (a) from GACOS method. (c) Corrected interferogram after subtracting (b) from (a). (d) is the original unwrapped coseismic interferogram from Sentinel-1 ascending track 128. (e) Modelled atmospheric phase delay for (d) from GACOS method. (f) Corrected interferogram after subtracting (e) from (d).

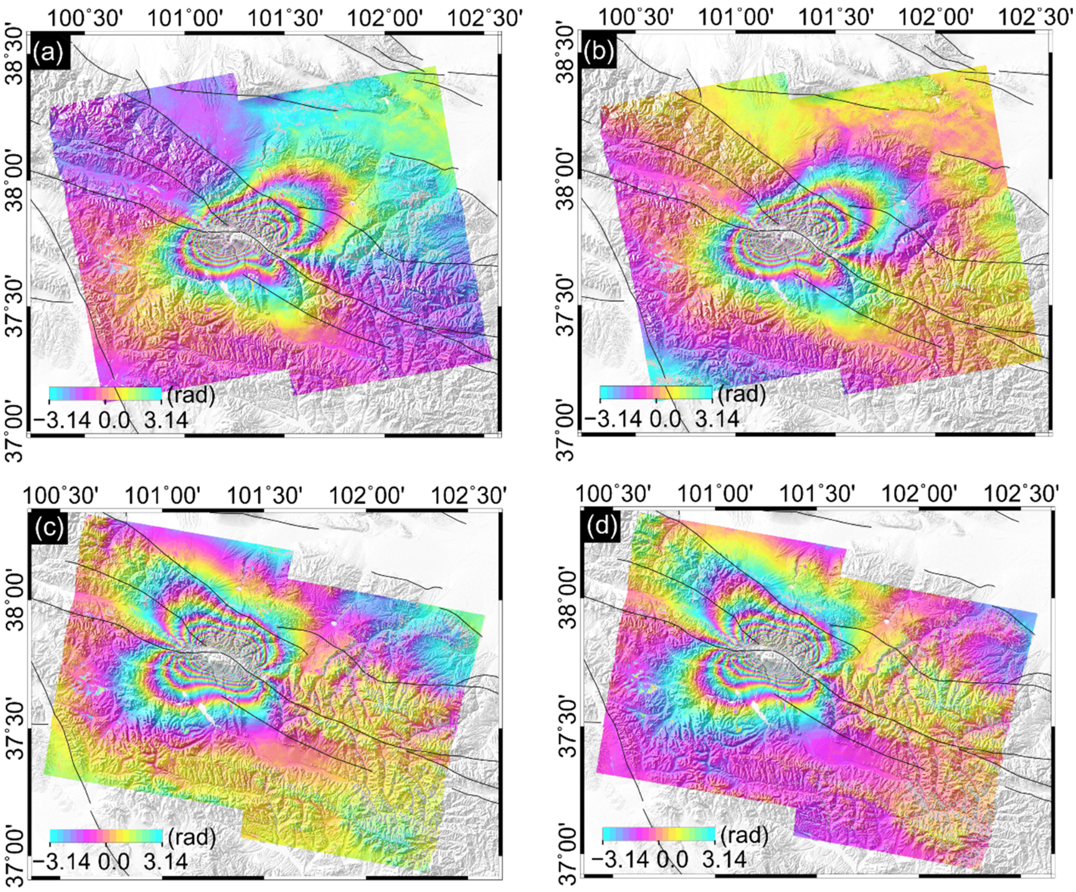

Figure S2. The orbit errors correction for descending track 33 and ascending tracking 128. (a) the original unwrapped coseismic interferogram of descending track 33. (b) the unwrapped interferogram after subtracting a first-order spatial non-deformed long-wavelength phase ramp from (a). (c) the original unwrapped coseismic interferogram of ascending track 128. (d) the unwrapped interferogram after subtracting a first-order spatial non-deformed long-wavelength phase ramp from (c).

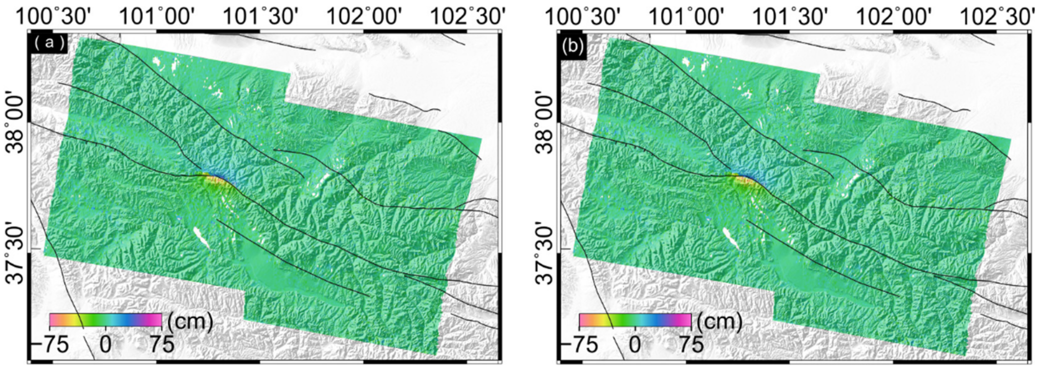

Figure S3. The long wavelength phase errors correction for the pixel offset tracking in range direction. (a) the original range offset tracking map of descending track 33. (b) the corrected range offset tracking map by subtracting the estimated first-order phase ramp.

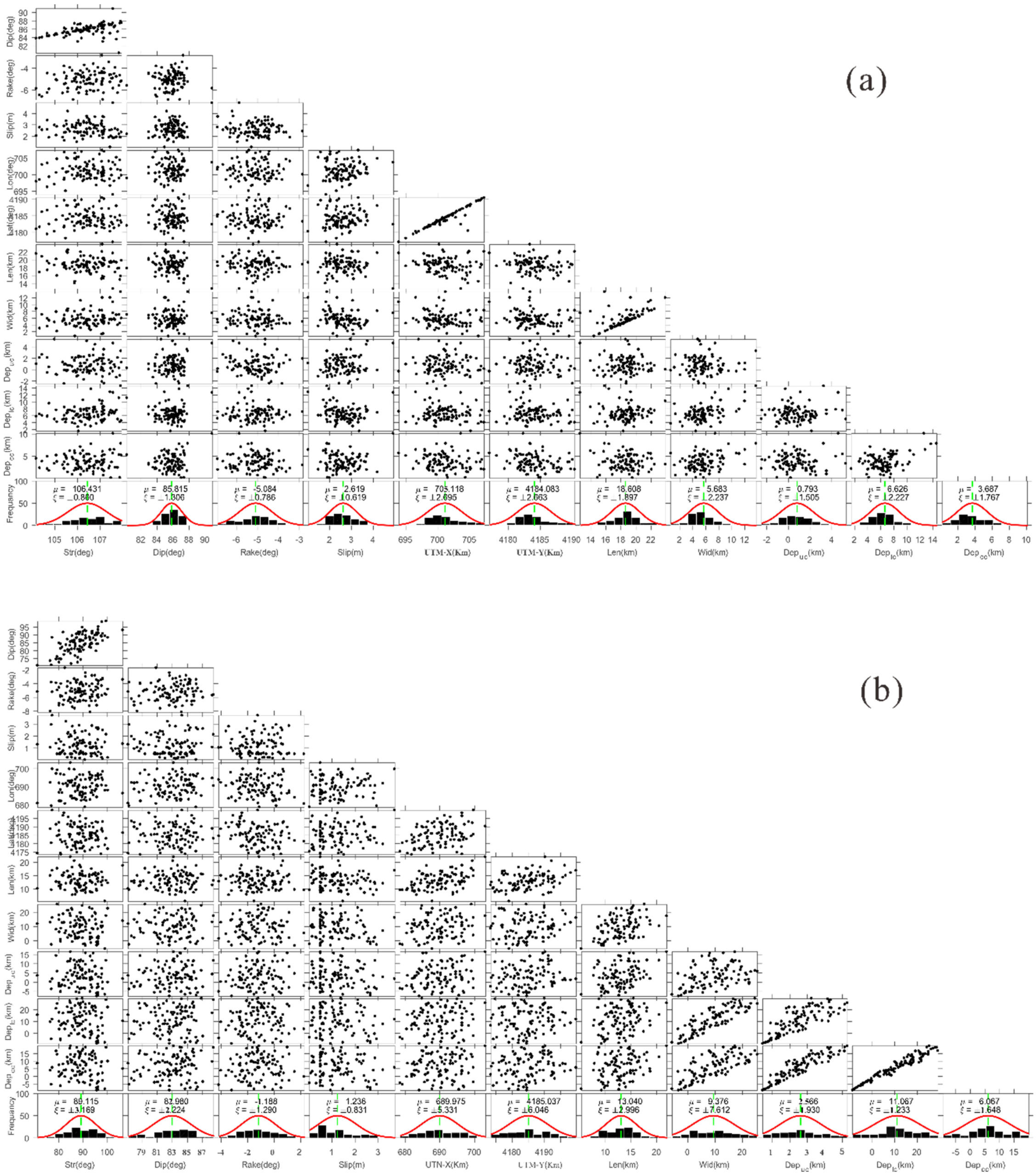

Figure S4. Uncertainties and trade-offs for the nonlinear inversion computed using Monte Carlo analysis. (a) the Monte Carlo analysis for F1. (b) Monte Carlo analysis for F2.

Table S1. Focal mechanisms and rupture parameters from different studies.

Source	Lon	Lat	Focal mechanism	Depth(km)	Mag. (Mw)
IPGP	101.275°E	37.811°N	284°/89°/-2°	15.0	6.68
USGS	101.278°E	37.815°N	104°/88°/15°	11.5	6.61
GCMT	101.31°E	37.80°N	104°/82°/1°	14.8	6.7
GFZ	101.34°E	37.81°N	285°/82°/16°	10.0	6.6
IG, CEA	101.26°E	37.77°N	109°/81°/39°	4.0	6.6
Li et al., 2022	-	-	F1: 104°/80°/0° F2: 109°/80°/5°	5.0	6.7
InSAR (This study)	101.28°E	37.812°N	F1: 106°/86°/-5° F2: 89°/83°/-1°	4.0	6.6

Table S2. SAR images used in the InSAR analysis

Track	Direction	Master	Slave	Spat. baseline	Inc. angle
26	ASC	20211229	20220110	107	45
33	DSC	20211229	20220110	55	38
128	ASC	20220105	20220117	39	36

Table S3. Parameters in the stratified viscoelastic Burgers model

Layer	Thickness/km	V_P/km·s^{-1}	V_S/km·s^{-1}	ρ/kg·m^{-3}	η_1/Pa·s	η_2/Pa·s
Upper crust	10	5.90	3.41	2500	—	
	10	6.18	3.57	2700		
Middle crust	12	5.85	3.38	2600	9.0×10^{18}	1.0×10^{19}
Lower crust	10	6.40	3.59	3000	9.0×10^{18}	1.0×10^{19}
	20	6.80	3.70	3100	9.0×10^{18}	1.0×10^{19}
Upper mantle		8.10	3.89	3350	0	1.0×10^{20}

V_P: P wave velocity, V_s :S wave velocity, ρ: density, η_1: transient viscosity coefficients, and η_2: steady-state viscosity coefficients.